JOURNAL OF VIROLOGY, July 1980, p. 76-92
0022-538X/80/07-0076/17$02.00/0

Vol. 35, No. 1

Functional Organization of the Harvey Murine Sarcoma Virus Genome

ESTHER H. CHANG,[1]* JEAN M. MARYAK,[2] CHA-MER WEI,[2] THOMAS Y. SHIH,[2] RALPH SHOBER,[2] HELEN L. CHEUNG,[3] RONALD W. ELLIS,[2] GORDON L. HAGER,[2] EDWARD M. SCOLNICK,[2] AND DOUGLAS R. LOWY[1]

Dermatology Branch[1] and Tumor Virus Genetics Branch,[2] National Cancer Institute, Bethesda, Maryland 20205, and Meloy Laboratories, Springfield, Virginia 22151[3]

The comparative infectivity of Harvey murine sarcoma virus (Ha-MuSV) DNA for NIH 3T3 cells was determined for supercoiled Ha-MuSV DNA molecularly cloned in λ phage and pBR322 at its unique *Eco*RI site (which is located near the middle of the 6-kilobase pair [kbp] unintegrated linear viral DNA) and for two cloned subgenomic fragments: one was 3.8 kbp and lacked about 1 kbp from each side of the *Eco*RI site, and the second did not contain the 3 kbp of the unintegrated linear viral DNA located on the 3′ side of the *Eco*RI site. Each subgenomic DNA induced foci of transformed cells, but with a lower relative efficiency then genomic DNA. Transfection with intact vector Ha-MuSV DNA yielded results similar to those obtained after separation of Ha-MuSV DNA from vector DNA. Cell lines were then derived from individual foci transformed with each type of viral DNA. Focus-forming virus was recovered from transformed cells after superinfection with a helper-independent virus, but the efficiency varied by several orders of magnitude. For several transformed lines, the efficiency of recovery of focus-forming virus was correlated with the structure of the Ha-MuSV DNA in the cells before superinfection. When ^{32}P-labeled Ha-MuSV DNA probes specific for sequences on either the 3′ or 5′ side of the *Eco*RI site were used to analyze the viral RNA in the transformed cell lines, all lines were found to hybridize with the 5′ probe, but some lines did not hybridize with the 3′ probe. The transformed lines contained high levels of the Ha-MuSV-coded p21 or its associated GDP-binding activity. We conclude that the transforming region and the sequences that code for the viral p21 protein are both located within the 2 kilobases closest to the 5′ end of the Ha-MuSV genome.

Harvey murine sarcoma virus (Ha-MuSV) and the closely related Kirsten (Ki)-MuSV belong to a class of mammalian type C retroviruses that are highly oncogenic in vivo, induce morphological transformation of fibroblasts in tissue culture, and are defective for replication (2, 19, 50; T. Y. Shih and E. M. Scolnick, *in* G. Klein, ed., *Viral Oncology*, in press). Superinfection of sarcoma virus-transformed cells with a type C helper-independent virus enables the transforming activity to be transmitted to uninfected cells, since these genomes can be efficiently pseudotyped ("rescued") by the virion proteins of a helper-independent virus.

Ha-MuSV and Ki-MuSV were originally isolated from tumors that developed in rats inoculated with a helper-independent retrovirus, Moloney murine leukemia virus (Mo-MuLV) for Ha-MuSV (20) and Ki-MuLV for Ki-MuSV (24). Ha-MuSV and Ki-MuSV are each recombinants between the helper-independent virus and rat cell nucleic acid sequences (38, 39); the 5.4-kilobase (kb) Ha-MuSV RNA genome is composed of an approximately 4.5-kb insert of rat genetic sequences flanked on the 5′ and 3′ ends by about 0.1 and 0.9 kb of Mo-MuLV sequences, respectively (5, 6, 45). Although Ha-MuSV does not synthesize any known Mo-MuLV translation products, it has recently been shown that transformation by Ha-MuSV (and by Ki-MuSV) is associated with the production of a 21K nonvirion phosphoprotein (p21), which is encoded by the viral genome (43). The p21 is required for maintenance of virus-induced transformation, since it is thermolabile in a mutant of Ki-MuSV that is temperature sensitive for the maintenance of transformation (44). It is not known what portion of the viral genome encodes the p21 protein, nor is it known whether the transforming function requires part or all of the viral genome.

It has been recognized for some time that retroviruses replicate through a viral DNA intermediate, but the unique structural organization of these viral DNAs has only recently been elucidated (22, 23, 35, 41). Three major forms of

viral DNA have been described: an unintegrated linear DNA intermediate, a covalently closed circular DNA intermediate, and the integrated viral DNA. The unintegrated linear form of viral DNA was found to be longer than the genomic RNA (exclusive of the 3'-terminal polyadenylic acid) because of direct terminal repetitions in the viral DNA. In addition to a colinear copy of the viral RNA, which contains a short direct terminal duplication (about 50 nucleotides in murine retroviruses [7]), the viral DNA contained sequences at the 5' end which were derived from the 3' end of the viral RNA, whereas sequences derived from the 5' end of the viral RNA were located at the 3' end of the viral DNA. For murine retroviruses, this extended terminal repetition (ETR) contained about 0.5 kb derived from the 3' end of the viral RNA and 0.15 kb derived from the 5' end of viral RNA (5, 13). The integrated viral DNA was colinear with the unintegrated linear DNA and contained ETR. The closed circular form of viral DNA was heterogeneous with respect to the ETR (52); some molecules, which were the same length as the viral RNA, contained only one copy of these sequences, whereas other supercoiled molecules contained tandem reiterations of these sequences.

We have recently reported the molecular cloning in λ DNA of Ha-MuSV supercoiled circular DNA intermediates linearized by *Eco*RI, which cleaved the viral DNA in a single site (18). Since the viral *Eco*RI site was located near the middle of the unintegrated linear viral DNA isolated from newly infected mouse cells (14, 18), the cloned viral DNAs were permuted with respect to the unintegrated linear viral DNA (see Fig. 1). Three size classes of Ha-MuSV DNA inserts were isolated: 5.4 (S clone), 6.0 (M clone), and 6.6 kilobase pairs (kbp) (L clone). Each molecule begins with the 3' half of the Ha-MuSV genome and continues through one or more copies of the ETR into the 5' half of the genome. The S clone contained the same sequences as genomic RNA, whereas the M and L clones contained a tandem duplication and triplication, respectively, of the

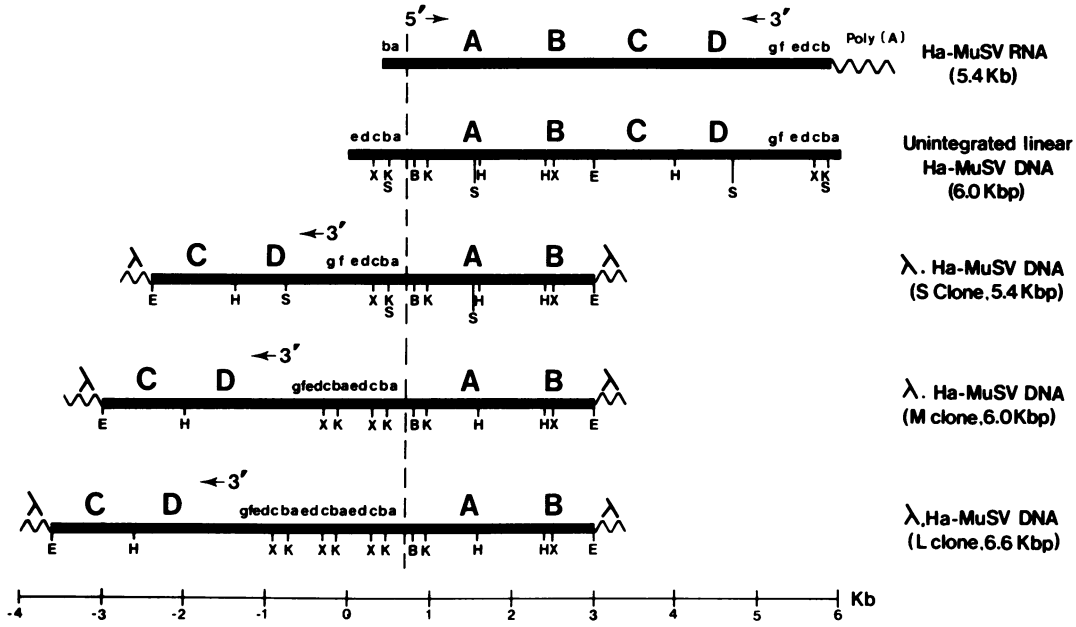

FIG. 1. *Structural relationship of λ·Ha-MuSV DNAs to viral RNA and to unintegrated linear viral DNA isolated from acutely infected mouse cells. The small capital letters (below each DNA) refer to restriction endonuclease sites: E = EcoRI, X = XbaI, K = KpnI, S = SmaI, B = BamHI, H = HindIII. The lower-case letters indicate the relative location of Mo-MuLV-derived sequences in the termini of the Ha-MuSV RNA and in the Ha-MuSV DNAs: a = those sequences contained exclusively at the 5' end of the viral RNA which are duplicated at the 3' end of the unintegrated linear viral DNA (at least some of these are rat-derived sequences); b = those sequences that are duplicated at both ends of the viral RNA; c, d, and e = those sequences contained exclusively at the 3' end of the viral RNA that are duplicated at the 5' end of the unintegrated linear viral DNA; f and g = sequences adjacent to e which are not duplicated in the viral DNAs. The large capital letters (above each viral RNA and DNA) refer to the relative order of the rat-derived sequences. The λ DNA arms have not been drawn to scale.*

ETR (5). After digestion with *Eco*RI, which separated Ha-MuSV DNA from λ DNA, molecules of all three size classes induced foci of transformed NIH 3T3 cells. After mass cultures which had been transformed by multiple independent transformation events were superinfected with a helper-independent virus, focus-forming virus (FFV) could be transmitted with high efficiency to uninfected cells.

In the present communication, we have begun to study the functional organization of the Ha-MuSV genome. We have molecularly cloned two subgenomic DNA fragments of Ha-MuSV, compared the transforming activity of these DNAs with that of the previously cloned viral DNA, studied the structure and expression of Ha-MuSV in the transformed cells, and correlated these findings with the ability to rescue FFV from the cells. In contrast to the 3′ location of the transforming (*src*) regions of Mo-MuSV (1) and Rous sarcoma virus (11, 50, 51), we have localized the transforming and p21-coding region of Ha-MuSV to the 5′ end of the viral genome.

MATERIALS AND METHODS

Cells and virus. The NIH 3T3 mouse embryo fibroblasts (25), XC rat cells (48), and NIH 3T3 cells chronically infected with Mo-MuLV and Ha-MuSV (29) have been described. Mo-MuLV clone 2 was obtained from Nancy Hopkins. It was endpoint diluted on and grown in NIH 3T3 cells.

Cells were grown in Dulbecco-modified Eagle minimal essential medium (Flow Laboratories) supplemented with penicillin (100 U/ml), streptomycin (100 μg/ml), and 10% heat-inactivated fetal bovine serum (Flow Laboratories). The cultures were negative for mycoplasma by aerobic and anaerobic techniques (Flow Laboratories).

Overnight culture fluids were assayed for virus on uninfected NIH 3T3 cells. Mo-MuLV and Ha-MuSV titers were determined by the XC plaque test (34) and by focus formation (25), respectively. Using these assays, the NIH 3T3 cells chronically infected with the leukemia-sarcoma virus mixture regularly titered about 10^7 PFU and focus-forming units (FFU) per ml, with a PFU to FFU ratio of about 2:1. The NIH cells chronically infected with Mo-MuLV titered about 10^7 PFU/ml.

Enzymes. Restriction endonucleases were obtained from Bethesda Research Laboratories and New England Biolabs and were used according to the supplier's assay conditions; occasionally, enzymes were used in an amount from 2 to 10 times that recommended for cleavage. T4 DNA ligase was purchased from Bethesda Research Labs and used under the standard conditions specified by the supplier.

Infectivity studies. The λgtWES·λB Ha-MuSV DNAs used were clone 10 (S; 5.4-kbp insert), clone 2 (M; 6.0-kbp insert), and clone 1 (L; 6.6-kbp insert) (18). Experiments were carried out according to the National Institutes of Health Guidelines for Recombinant DNA Research. The unintegrated linear Ha-MuSV DNA was obtained after agarose gel electrophoresis of Hirt supernatant DNA isolated from the NIH cells acutely infected with Mo-MuLV and Ha-MuSV (27). Transfections were carried out by the calcium precipitation method (15), as previously described (27). High-molecular-weight DNA isolated from NIH 3T3 cells or from calf thymus by the proteinase K method (16) was used as carrier DNA at 25 μg/ml. Both carrier DNAs gave similar infectivity results. The agarose gel electrophoresis infectivity study was performed as previously described (18).

For the derivation of cells nonproductively transformed by Ha-MuSV virus, NIH 3T3 cells were infected at limiting dilution with the sarcoma-leukemia virus complex derived from the chronically infected mouse cells. Because of the 2:1 helper virus ratio, the newly infected cells were grown under an agar overlay to prevent spread of Mo-MuLV through the culture.

Clonal lines of transformed cells derived from independent foci were obtained in the following manner. After transfection with viral DNA or infection with virus, transformed cells from individual foci were isolated from dishes containing fewer than five foci; only one focus was chosen from any dish. Each focus was isolated with a cloning cylinder, trypsin was added to the cylinder, and cells were gently removed by aspiration and transferred to a fresh dish. After one or two passages, cells from each focus were biologically cloned as single cells in microtiter wells. These clonally derived nonproducer cell lines were then used for the nucleic acid studies, for p21 and GDP-binding assays, and for the transmission of Ha-MuSV to uninfected cells.

For the transmission of Ha-MuSV, the transformed cells were superinfected with Mo-MuLV. Dishes (60-mm) that had been seeded the previous day with 10^5 transformed cells were infected with Mo-MuLV clone 2 at a multiplicity of infection of 0.1. Six days later, culture fluid, which had been added to the cells 18 h previously, was removed, clarified by low-speed centrifugation, filtered, stored at −70°C, and assayed on NIH 3T3 cells for Mo-MuLV and Ha-MuSV as noted above.

Agarose gel electrophoresis and DNA transfer. High-molecular-weight DNA was isolated from mouse cells (16), and λ·Ha-MuSV DNA was isolated from banded phage by established methods (18). Analytical electrophoresis of DNA samples was carried out as described (18, 42). Those lanes with high-molecular-weight DNA contained 15 μg of restriction endonuclease-digested DNA. Wild-type λ DNA cleaved with *Hin*dIII and end-labeled with [α-^{32}P]-dCTP, and *Hae*III-digested φX174 DNA, were used as markers. DNA to be hybridized with [^{32}P]DNA probes was transferred from the gel to nitrocellulose filters by the procedure of Southern (46) with minor modification.

Hybridization reagents and conditions. For DNA:DNA filter hybridization and for DNA:RNA liquid hybridization studies, gel-purified DNA was labeled with ^{32}P in vitro using the repair synthesis ("nick-translation") reaction of *Escherichia coli* DNA polymerase (30). The reaction used 100 μCi each of [α-^{32}P]dCTP and [α-^{32}P]TTP (New England Nuclear Corp., >300 Ci/mmol), and the specific activity of the

double-stranded [^{32}P]DNA probes was $\geq 10^8$ cpm/μg.

Two different Ha-MuSV probes were used for filter hybridization. The first was a representative probe, which was synthesized from the clone H-1 DNA. The second probe contained sequences corresponding to the 3.2 kbp in the unintegrated linear viral DNA from the *Sma*I site located 1.5 kbp from the 5′ end through the *Eco*RI site to the *Sma*I site located 1.3 kbp from the 3′ end (see Fig. 1). It therefore did not contain the Mo-MuLV sequences found in Ha-MuSV. This second probe was isolated by agarose gel electrophoresis of *Sma*I + *Eco*RI-digested clone H-1 DNA (S). After the two bands containing the sequences were isolated by electroelution (31), this DNA was re-electrophoresed, electroeluted, and pooled at a 1:1 ratio before being used to synthesize the ^{32}P probe. The λ[^{32}P]DNA was synthesized from λgtWES·λB DNA. The filters were hybridized with [^{32}P]DNA as previously described (18).

For DNA:RNA hybridization in liquid, cellular RNA was isolated from mouse cells as described (28). Two DNA probes were derived. They were synthesized by nick-translation from restriction endonuclease fragments of clone H-1 isolated from twice-electrophoresed DNA as described above. One, a 3′-specific piece, was the 3.0-kbp fragment containing the sequences from the *Eco*RI site to the *Kpn*I site located 0.1 kbp from the 3′ end of the unintegrated linear viral DNA (see Fig. 1). The other, a 5′-specific probe, was the 2.1-kbp fragment from the *Kpn*I site located 0.9 kbp from the 5′ end of the unintegrated linear viral DNA to the viral *Eco*RI site. Both DNA fragments were shown to be specific for their respective sequences by hybridization of blotted *Eco*RI + *Kpn*I-digested λ·Ha-MuSV DNA (M) to the nick-translated [^{32}P]DNA fragments. The reaction conditions for the DNA:RNA hybridizations are given in Results.

Transformation of *E. coli* with pBR322. Transformation experiments with the certified plasmid pBR322 (3) were performed according to a procedure developed by R. Curtiss (personal communication). In a typical experiment, 0.25 μg of Ha-MuSV insert was ligated to 0.25 μg of appropriately cut pBR322. *E. coli* RR-I (8; provided by H. W. Chan) cells were grown overnight in L-broth supplemented (per ml) with 100 μg of diaminopimelic acid, 50 μg of thymidine, 10 μg of biotin, and 1 μg of thiamine hydrochloride. Exponential-phase cells were washed and suspended in 75 mM $CaCl_2$ and 10 mM Tris-hydrochloride (pH 8.0). Cells were held in this buffer for 20 min, pelleted by centrifugation for 10 min at 500 × *g*, and resuspended in the same buffer at an approximate concentration of 3 × 10^8 cells per ml. The cells were held at 4°C for 2 min before mixing with the plasmid DNA. A 50-ng sample of DNA was then diluted in 100 μl of buffer containing 137 mM NaCl and 20 mM Tris-hydrochloride (pH 8.0). To each DNA preparation, approximately 6 × 10^7 cells were added in a volume of 200 μl. The mixtures were held at 4°C for 20 min, heated at 42°C for 1.5 min, and cooled in a room-temperature water bath for 10 min. The samples were then diluted 1:10 in L-broth plus supplements (as described above) and incubated at 37°C for 90 min with shaking. Cultures were then plated for overnight growth at various dilutions on 1.2% agar plates containing L-broth, growth medium supplements, and the appropriate antibiotic for selection. Colony hybridization (17) was performed using Ha-MuSV ^{32}P-labeled complementary DNA for the selection of virus-containing clones. Large quantities of purified recombinant DNA were prepared by Hirt supernatant extraction (21) of DNA from cell pellets and hydroxyapatite chromatography (9).

Molecular cloning in λ of 5′ Ha-MuSV clone. Hirt supernatant viral DNA was isolated from mouse cells newly infected with the Mo-MuLV pseudotype of Ha-MuSV (27). The 6.0-kbp unintegrated linear Ha-MuSV DNA was selected by RPC-5 chromatography (33) and identified by the Southern (46) blotting technique using Ha-MuSV ^{32}P-labeled complementary DNA. The fractions that contained the linear viral DNA were pooled, and DNA was made fully double-stranded by treatment with *E. coli* DNA polymerase (Sigma). After double-stranded DNA octomers which contained the *Eco*RI recognition sequences (Collaborative Research) were ligated to the viral DNA, it was digested with *Eco*RI. The digested linkers were then removed by sucrose gradient centrifugation. The viral DNA was then ligated to the arms of the λgtWES·λB (26) DNA EK-2 cloning vector, packaged, and amplified (18).

RESULTS

Cloning of Ha-MuSV subgenomic fragments. The Ha-MuSV (S clone) insert and a defined fragment of this insert were subcloned in the plasmid vector pBR322. The pBR322 clone containing the complete S clone insert (clone H-1 in Fig. 2) was derived by digestion of

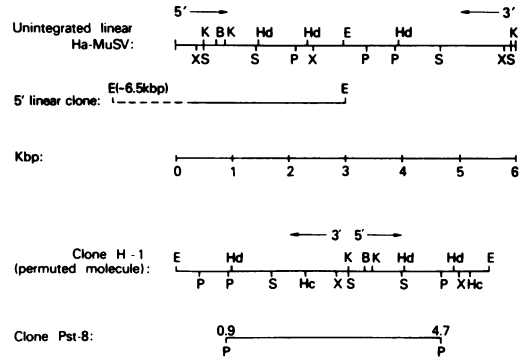

FIG. 2. *Schematic representation of Ha-MuSV: unintegrated linear molecule, the cloned permuted molecule, and the cloned subgenomic fragments. Major restriction enzyme sites are indicated on the unintegrated linear and permuted molecules, as well as at the ends of the cloned fragments. The key to the enzymes used is as in Fig. 1, except that Hd = HindIII, Hc = HincII, and P = PstI. A scale of kilobase pairs (kbp) is given in the center of the diagram. The map position of the fragments is indicated by their placement on the diagram, as well as by map positions (in kbp) and restriction sites at their ends. The 5′-linear clone, in addition to the 5′ half of Ha-MuSV DNA, contains 6.5 kbp of nonviral DNA.*

λ·Ha-MuSV (S clone) with *Eco*RI, separation of the insert from the λ arms by centrifugation on a sucrose density gradient, and ligation of the Ha-MuSV insert to *Eco*RI-digested pBR322. For isolation of the subgenomic Pst-8 clone (Fig. 2), purified Ha-MuSV insert was digested with *Pst*I and ligated to *Pst*I-digested pBR322. Restriction analysis of these DNAs has revealed the expected cleavage products (Table 1).

The second subgenomic fragment was located at one end of a 9.5-kbp insert cloned in λ DNA. The viral sequences in this insert included only the 3 kbp located on the 5′ side of the *Eco*RI site of the unintegrated linear viral DNA (the 5′ linear clone in Fig. 2). In the insert, these viral sequences were fused at or near the termination of the ETR to 6.5 kbp of nonviral mouse sequences. This clone was derived from Hirt supernatant DNA isolated from mouse cells acutely infected with an Mo-MuLV pseudotype of Ha-MuSV. This DNA was first enriched for the unintegrated linear viral DNA by RPC-5 chromatography, and the fractions containing the 6.0-kbp Ha-MuSV were made flush-ended with *E. coli* DNA polymerase I. *Eco*RI linkers were ligated to this DNA, which was then digested with *Eco*RI. Since the unique *Eco*RI site in Ha-MuSV is located near the middle of the unintegrated linear viral DNA, this procedure was designed to cleave the viral DNA into a 5′ half and a 3′ half, each with *Eco*RI termini. After ligation of this DNA preparation to the *Eco*RI arms of λ DNA and amplification in *E. coli*, the 5′ half was isolated, but as noted above, it was fused to nonviral DNA. Since the viral DNA was initially size selected, and this 9.5-kbp insert did not contain an *Eco*RI site between the viral and nonviral DNA, it is most likely that the insert ligation of these two DNAs arose after inadvertent ligation of these two DNAs during the cloning process, although the possibility that it arose from integrated viral DNA cannot be formally excluded. The identity of the 3 kbp of viral DNA in the insert has been verified by extensive restriction enzyme analysis, molecular hybridization of the Southern blotted cleavage products with Ha-MuSV [^{32}P]DNA, and comparison of the results with the cleavage products of the unintegrated linear Ha-MuSV DNA (Table 1).

TABLE 1. *Restriction digests of Ha-MuSV DNA inserts*

Restriction endonuclease	Size (kbp) of digests[a]			
	Unintegrated linear Ha-MuSV[b]	Clone H-1[c]	5′-linear clone[d]	Clone Pst-8[c]
*Bam*HI	0.8, 5.2	3.3, 2.2	*1.8*, 2.2	2.4, 1.4
*Eco*RI	3.0, 3.0	5.5	*9.5*	3.8
*Hin*cII	ND[e]	2.3, 2.9, 0.3	*3.5*, 0.3	1.3, 2.5
*Hin*dIII	1.6, 0.9, 1.6, 2.0	1.0, 3.0, 0.9, 0.6	*7.4*, 0.9, 0.6	3.0, 0.7
*Kpn*I	0.5, 0.4, 5.0	3.0, 0.4, 2.1	*4.3*, 0.4, 2.1	2.1, 0.4, 1.3
*Pst*I	ND[f]	0.5, 0.4, 3.8, 0.8	ND	3.8
*Sma*I	0.5, 1.0, 3.2, 1.3, 0.1	1.7, 1.3, 1.0, 1.5	*0.9*, 1.0, 1.5	0.8, 1.3, 1.0, 0.7
*Xba*I	0.3, 2.2, 3.3, 0.3	2.8, 2.2, 0.5	*6.8*,[g] 2.2, 0.5	1.9, 1.9

[a] Each set of digests is listed in its left-to-right order as shown in Fig. 2. The sizes of the digests have been rounded to the nearest 0.1 kbp.

[b] Unintegrated linear nonpermuted Ha-MuSV DNA was isolated from the Hirt supernatant of acutely infected cells. Sizes of digests were judged after Southern transfer and hybridization with Ha-MuSV ^{32}P-labeled complementary DNA.

[c] The sizes of these cloned DNA digests were judged after ethidium bromide staining.

[d] The sizes of digests hybridizing to clone H-1 [^{32}P]DNA after Southern transfer are listed. All italicized numbers represent digest sizes that are not found in H-1 and, therefore, consist of both Ha-MuSV and cellular DNA seqeunces.

[e] ND, Not done.

[f] According to Goldfarb and Weinberg (14), the results are 2.25, 2.1, 1.2, and 0.5 kbp.

[g] The usually weak hybridization of the probe to this DNA fragment (data not shown) suggests that Ha-MuSV sequences terminate within a short distance of the left side (as shown in Fig. 2) of the *Xba*I site near the middle of the H-1 clone. This conclusion is supported by the absence in the clone of the *Hin*cII site 0.6 kbp on the left side of *Xba*I.

Transforming activity of Ha-MuSV DNA. In the initial studies of the λ·Ha-MuSV DNA (18), the infectivity of the recombinant DNA preparations was tested only after the DNAs had been digested with *Eco*RI, the enzyme which had been used to clone the viral DNA. A recent change in the National Institutes of Health Guidelines for Recombinant DNA Research also permitted the infectivity of uncut hybrid DNAs to be assayed in mouse cells (10). If focus formation were induced with undigested cloned DNAs with an efficiency similar to that obtained with digested DNA, the results would suggest that transfected DNA could induce transformation in its cloned permuted orientation without reorientation of the viral DNA. Therefore, when the ability of the recombinant DNA clones to transform NIH cells was tested, each DNA was assayed both undigested from its vector and after digestion with the enzyme used to clone the DNA.

Table 2 summarizes the data from several experiments involving the Ha-MuSV genome cloned in λ and in pBR322 and the subgenomic fragments. Each recombinant clone induced focal transformation of the NIH cells (experiments I, II, and III). Since the 5′-linear clone induced foci, it was clear that the 3 kbp on the 3′ side of the *Eco*RI site of the unintegrated linear viral DNA were not absolutely required for the induction and maintenance of transformation. In

TABLE 2. *Infectivity of Ha-MuSV DNAs*

Expt	Source of DNA	Enzyme	Foci per μg of viral DNA	Relative infectivity[a]
I	L clone	Uncut	2.2×10^3	0.24
	L clone	*Eco*RI	6.4×10^3	0.71
	M clone	Uncut	1.9×10^3	0.21
	M clone	*Eco*RI	3.7×10^3	0.41
	S clone	Uncut	2.1×10^3	0.23
	S clone	*Eco*RI	9.0×10^3	1.00
II	S clone	Uncut	2.0×10^3	3.1
	S clone	*Eco*RI	1.5×10^3	3.9
	Clone H-1	Uncut	6.1×10^2	0.95
	Clone H-1	*Eco*RI	6.4×10^2	1.00
	Clone H-1	*Sal*I	7.0×10^2	1.09
	Clone Pst-8	Uncut	82	0.13
	Clone Pst-8	*Pst*I	51	0.08
	Clone Pst-8	*Sal*I	43	0.07
III	S clone	*Eco*RI	2.9×10^3	1.0
	5′-Linear clone	Uncut	48	0.02
	5′-Linear clone	*Eco*RI	77	0.03

[a] In experiments I and III, the infectivity of the *Eco*RI-digested S clone DNA was used as the standard (=1.00). In experiment II, the infectivity of *Eco*RI-digested clone H-1 was used as the standard (=1.00).

addition, the infectious clone Pst-8 lacked the 0.8 kbp between the *Pst*I site on the 5′ side of the viral DNA and the *Eco*RI site. This clone further localized the transforming region to the approximately 2.3 kbp of 5′ sequences located to the left of this *Pst*I site (see Fig. 2).

Although each DNA induced foci, each clone has its characteristic relative transforming efficiency. As previously reported (18), the specific infectivity of *Eco*RI-digested λ·Ha-MuSV DNA of all three size molecules was similar. This result indicated that the presence of tandem copies of the ETR did not significantly affect the infectivity of the Ha-MuSV DNA. The specific infectivity of the Ha-MuSV insert was consistently higher in λ than in its pBR322 subclone. The transforming activity of the two subgenomic fragments was one to two orders of magnitude lower than that of the complete genome. These results suggested that although the sequences on the 3′ side of the *Pst*I site were not absolutely required for the induction of transformation, their presence (even in the permuted orientation of the cloned Ha-MuSV genome) enhanced the ability of the DNA to induce transformation in this transfection assay.

The transfection results also show that it made little difference whether the DNA was cleaved from the vector or transfected intact. Digestion of clones H-1 and Pst-8 and *Sal*I, which cleaves pBR322 once and does not cleave Ha-MuSV, also had no significant effect on the infectivity of this clone (experiment II). To rule out the possibility that the infectivity of the undigested recombinant DNA might be due to broken fragments of DNA in the preparation, undigested and *Eco*RI-digested λ·Ha-MuSV (S) DNA were electrophoresed in adjacent lanes of an agarose gel, and the focus-inducing activity of gel slices from each lane was assayed in NIH cells (Fig. 3). As previously reported, the infectivity of the *Eco*RI-digested DNA resided in the Ha-MuSV DNA insert (5.4 kbp). By contrast, the infectivity of the undigested DNA, as expected for an intact molecule, was confined to the region of the gel that contained the undigested recombinant DNA.

Viral RNA in transformed cell lines. Having localized the transforming regions to a specific segment of the viral DNA, it was of interest to correlate these findings with the viral RNA found in the transformed cells. We have therefore assessed the RNA expression of defined regions of the viral genome in cells transformed by the different recombinant DNAs. Double-stranded ^{32}P probes specific for sequences located on the 5′ and 3′ sides of the Ha-MuSV *Eco*RI site were obtained from defined fragments of the cloned DNA. The viral sequences represented in each probe are shown in Fig. 4. The specificity of each [^{32}P]DNA probe was determined using the stringent conditions of probe excess, although the RNA hybridizations were carried out under the less rigorous conditions of substrate excess. The cell RNA was isolated from transformed lines which had been

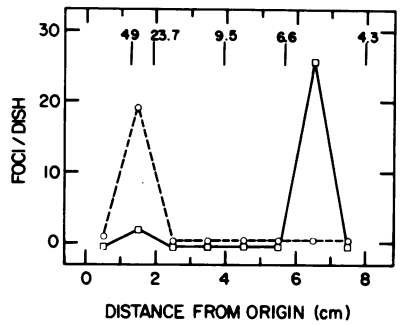

FIG. 3. *Infectivity of agarose gel electrophoresis fractions of undigested and EcoRI-digested λ·Ha-MuSV DNA (S clone). Samples of 4 μg of recombinant DNA were subjected to electrophoresis in a 1% agarose gel at 30 V for 72 h. Ten percent of each gel slice was used for the infectivity assay (27). The vertical bars and the numbers above them indicate the location and length (in kilobase pairs), respectively, of HindIII-digested wild-type λ DNA run in an adjacent lane.* (○) *Undigested DNA;* (□) *EcoRI-digested DNA.*

derived from single-cell clones of independently induced foci.

RNA from all the lines transformed with the complete viral genome or with the 5′ linear clone hybridized extensively (≥80%) with the 5′ probe (Table 3). As expected, RNA from a line transformed with clone Pst-8 hybridized less extensively (57%), since the *PstI* subgenomic fragment in this clone contained only 60% of the sequences in the 5′ probe. The kinetics of hybridization are shown for some representative lines (Fig. 4A). There was little difference (<threefold) between the level of 5′ RNA expression in cells transformed with Ha-MuSV virus and those transformed with the cloned DNAs.

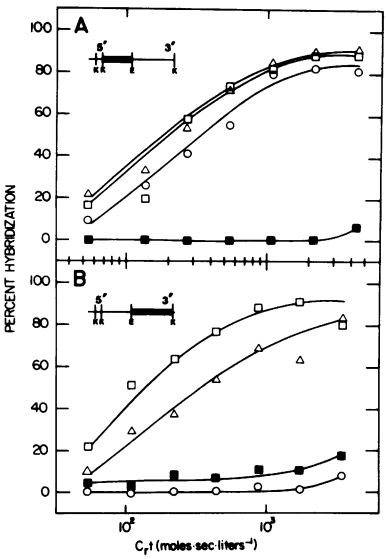

FIG. 4. *Hybridization of transformant cell RNA to [^{32}P]DNA specific for the 5′ and 3′ regions of Ha-MuSV. The DNA probes were synthesized as described in the text. Each hybridization reaction was incubated at 66°C for 24 h and contained in 0.05 ml: 0.02 M Tris-hydrochloride (pH 7.5), 0.75 M NaCl, 0.001 M EDTA, 0.1% sodium dodecyl sulfate, 10 μg of carrier yeast RNA, the indicated RNA sample, and about 5,000 trichloracetic acid-insoluble counts per minute of [^{32}P]DNA. After S1 nuclease digestion, the number of trichloroacetic acid-insoluble counts per minute was determined. In the absence of added RNA, less than 5% of the input counts were resistant to S1 nuclease. Maximum hybridization to Ha-MuSV RNA (1,220 net cpm for the 5′ probe and 1,259 net cpm for the 3′ probe) was considered to be 100%, and other results were normalized to this value. Hybridization results were analyzed as a function of time and RNA concentration and expressed as C_rt (moles per liter times second). (A) Hybridization to the 5′ probe; (B) hybridization to the 3′ probe. The DNA sequences contained in each probe are shown schematically by the heavy line in the unintegrated linear viral DNA in each panel. (■) Uninfected cells; (□) virus-transformed nonproducer (focus 19). EcoRI-digested S clone transformants: (△) focus 9, high rescue, and (○) focus 15, low rescue.*

In contrast to the uniformly extensive hybridization seen with the 5′ probe, the results obtained with the ^{32}P-labeled Ha-MuSV 3′ probe were strikingly heterogeneous (Table 3, Fig. 4B). The results from most lines fell into one of two categories: the RNA either hybridized extensively (≥80%) or it did not hybridize to a greater extent than did RNA from uninfected cells. As expected, the lines transformed with Ha-MuSV virus and with in vivo-derived intact unintegrated linear viral DNA contained the 3′ RNA, whereas the cells transformed with the 5′ linear clone (which lacks the 3′ half of the genome) lacked this class of RNA. It should also be noted that some lines transformed with *Eco*RI-di-

TABLE 3. *Hybridization of RNA from nonproductively transformed cells to 3′- and 5′-specific probes*[a]

Source of RNA	Ha-MuSV 5′ probe		Ha-MuSV 3′ probe	
	cpm	% Hybrid	cpm	% Hybrid
Ha-MuSV viral RNA	1,220	100	1,259	100
Uninfected cells	92	8	243	19
Cells transformed by:				
Ha-MuSV virus				
Focus 13	1,160	95	1,298	100
Focus 19	1,107	91	1,180	94
Unintegrated linear Ha-MuSV DNA				
Focus 7	1,126	92	1,201	95
Focus 8	1,022	84	1,187	94
Undigested λ·Ha-MuSV DNA				
Focus 20a (from S clone)	1,122	92	1,115	89
Focus 20b (from S clone)	1,241	100	662	53
Focus 28 (from M clone)	974	80	1,005	80
*Eco*RI-digested λ·Ha-MuSV DNA				
Focus 14 (from S clone)	1,224	100	172	14
Focus 15 (from S clone)	1,126	92	100	8
Focus 27 (from M clone)	961	79	245	19
Focus 9 (from S clone)	1,137	93	1,063	85
Focus 22 (from S clone)	1,197	98	1,046	83
Focus 36 (from M clone)	1,206	99	1,064	85
*Eco*RI-digested 5′-linear clone				
Focus 4a	1,047	86	130	10
Undigested clone Pst-8				
Focus 2	695	57	653	52

[a] Hybridization reactions were performed as described in Fig. 4. The net ^{32}P counts per minute (cpm) given represents the maximum obtained for each RNA at $C_rt \geq 3 \times 10^3$.

gested λ·Ha-MuSV DNA fell into each of the two hybridization categories. The lines transformed with undigested recombinant DNA contained significant levels of some 3′ RNA sequences.

These molecular hybridization results therefore confirmed the transfection data presented in the previous section, since the DNA:RNA hybridizations also indicated that expression of the sequences on the 3′ side of the *PstI* site located in the 5′ half of the viral DNA was not required for maintenance of the transformed phenotype. Since the 3′ probe included the sequences of the ETR that were derived from the 3′ end of the viral RNA, the data also demonstrated that transformation was maintained in the absence of RNA expression of the sequences in the ETR which were derived exclusively from the 3′ end of the viral RNA (c, d, and e in Fig. 1).

The presence of p21 in transformed cell lines induced by DNA clones. As noted earlier, the region of the viral genome that contains the sequences encoding the viral p21 has not yet been established. The lines transformed with the cloned DNAs have enabled us to ascertain whether the p21 coding sequences are located within the transforming region of the viral genome. A GDP-binding activity has recently been found to be associated with the p21; the binding of [^{3}H]GDP to this protein forms the basis of an assay which simplifies and specifies the identification of p21 (37). In this assay, unlabeled extracts from transformed cells are incubated with [^{3}H]GDP; picomole quantities of the nucleotide are bound and can be immunoprecipitated with antisera to p21. We have assessed the presence of p21 and its GDP-binding activity in extracts of several transformed cell lines whose viral RNAs were determined in the previous section.

Table 4 summarizes the GDP-binding results obtained with normal and immune sera. Whereas uninfected NIH 3T3 cells showed no binding, strong binding with the immune serum was found for all the transformants, including lines transformed with Ha-MuSV virus, clone Pst-8, and the 5′ linear clone. Among the lines transformed with *Eco*RI-digested λ·Ha-MuSV, the GDP-binding activity was at least as high in the two lines that expressed only 5′ RNA sequences (foci 14 and 15) as in the two lines that also expressed the 3′ sequences (foci 9 and 22).

To further compare the p21 in the DNA transformants with the protein in a virus transformant, [^{35}S]methionine-labeled proteins from a line transformed with clone Pst-8 and from a line transformed with *Eco*RI-digested λ·Ha-MuSV (focus 14, which only expressed the 5′ sequences) were immunoprecipitated with antisera and subjected to polyacrylamide gel electrophoresis. In the autoradiogram of this experiment, both lines transformed with the cloned DNAs (C and D in Fig. 5) contained an intense Ha-MuSV-specific band which comigrated with the p21 of a virus-transformed nonproducer line (B in Fig. 5).

The p21 of cells transformed with the cloned DNA was therefore indistinguishable from the protein found in virus-transformed cells. Since even those lines that expressed only the 5′ RNA contained the p21, it was concluded that the p21 coding region must lie within the transforming region of the virus, i.e., within the 5′ half of the viral genome.

TABLE 4. *GDP-binding assay of the p21 protein in cells transformed by Ha-MuSV DNA*[a]

Form of Ha-MuSV that transformed the cells	[^{3}H]GDP bound (pmol)	
	Anti-serum	Normal serum
Uninfected cells		
NIH 3T3, low cell density	0.09	0.08
NIH 3T3, high cell density	0.10	0.06
Ha-MuSV virus		
Ha821	0.69	0.06
Focus 19	0.84	0.06
Unintegrated linear Ha-MuSV DNA		
Focus 7	0.68	0.05
Undigested λ·Ha-MuSV DNA (S clone)		
Focus 20a	0.83	0.07
Focus 20b	0.65	0.05
*Eco*RI-digested λ·Ha-MuSV DNA (S clone)		
Focus 14	0.84	0.05
Focus 15	0.56	0.08
Focus 9	0.53	0.08
Focus 22	0.42	0.06
Undigested clone Pst-8		
Focus 2	0.47	0.07
*Eco*RI-digested 5′-linear DNA		
Focus 4a	0.55	0.08
Focus 4b	0.67	0.09

[a] Cells were lysed in buffer containing 1% Triton X-100, 5 mM $MgCl_2$, 100 mM NaCl, 0.02 M Tris-hydrochloride (pH 7.4), and 200 U of Trasylol per ml, and protein concentration was determined by Lowry's method. Each binding assay mixture (300 μl) at 4°C contained 400 μg of protein, 0.01 mM [^{3}H]GDP (10 Ci/mmol), and 7 μl of heat-inactivated (56°C, 30 min) Ha-MuSV antiserum or normal rat serum. The antigen-antibody complexes and the bound [^{3}H]GDP were precipitated by 50 μl of formaldehyde-fixed *Staphylococcus aureus* suspension (10%, vol/vol). After washings, the radioactivity of bound [^{3}H]GDP was determined by liquid scintillation counting. Under present conditions, 7,300 cpm represented 1 pmol of [^{3}H]GDP. Values listed in the table are the average of duplicate determinations of each extract.

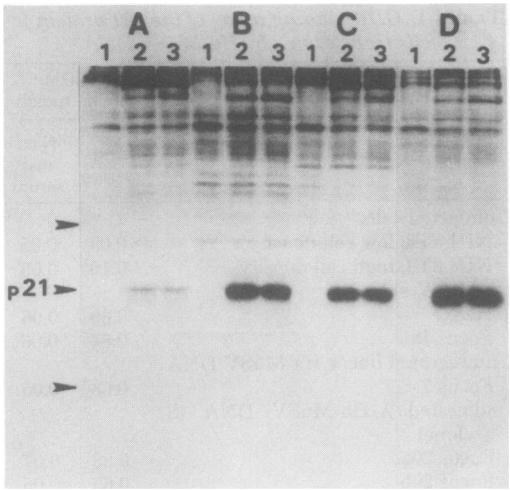

FIG. 5. *Immunoprecipitation of the p21 protein of Ha-MuSV DNA transformants. Cells were labeled with [^{35}S]methionine at 37°C for 4 h, and extracts were prepared and immunoprecipitated as described (43). The precipitated proteins were subjected to electrophoresis in 13% sodium dodecyl sulfate-polyacrylamide slab gels. The markers indicated by arrows were 30,000-dalton carbonic anhydrase (upper) and 14,000-dalton lysozyme (lower). Fluorography was for 18 h. Cells were (A) uninfected NIH 3T3 cells; (B) Ha-MuSV virus-transformed cells (Ha821); (C) Pst-8-transformed cells (focus 2); (D) EcoRI-digested S clone DNA-transformed cells, (focus 14, low rescue). Sera were (1) normal rat serum; (2) Ha-MuSV antiserum 1; (3) Ha-MuSV antiserum 2.*

Rescue of FFV from Ha-SV DNA-transformed cells. As noted in the Introduction, when cells nonproductively transformed by a sarcoma virus are superinfected with a helper virus, the sarcoma viral genome is pseudotyped (rescued) by the helper virus proteins, which enables fluid from infected cells to transmit the sarcoma virus to uninfected cells.

The relative contribution of different regions of the sarcoma viral genome to the transmission of focus formation by this mechanism has been unclear. Since focus formation by virus requires at least one cycle of viral replication, it seemed likely that viral sequences, in addition to the transforming sequences, might significantly affect the transmission of focus formation. Testing the efficiency with which sarcoma virus (as measured by focus formation on uninfected NIH 3T3 cells) could be recovered after superinfection of the transformants with Mo-MuLV might therefore provide some further insight into the biological function of regions other than the p21 coding sequence.

We first tested the ability to rescue FFV from mass cultures (consisting of cells derived from at least 50 different foci) which had been transformed with the permuted Ha-MuSV in λ and pBR322 and with clone Pst-8 before and after their digestion with the enzyme used to clone the DNA. The focus-forming activity of supernatant fluids was determined 6 days after superinfection with Mo-MuLV (Table 5). As previously reported (18), FFV was rescued with high efficiency ($10^{5.9}$ FFU/ml) from the culture transformed with *Eco*RI-digested λ·Ha-MuSV DNA. By contrast, the FFV titer from the undigested λ·Ha-MuSV was more than four orders of magnitude lower ($10^{1.3}$). For clone H-1 (which is a circular molecule, in contrast to the linear λ S clone), the FFV titer from cells transformed with undigested molecules was only about one order of magnitude lower than from the culture transformed with *Eco*RI-digested molecules ($10^{4.7}$ versus $10^{6.0}$). However, when clone H-1 was linearized with *Sal*I, FFV titer was similar to that seen with the undigested λ S clone. FFV was also rescued from the cultures transformed from clone Pst-8, but with lower titers than with the comparable form of clone H-1. Since clone Pst-8 lacks 1.7 kbp of the rat-derived Ha-MuSV sequences, these FFV must differ from wild-type Ha-MuSV at least with respect to these sequences. The missing sequences in Pst-8 were not absolutely required for recovery of FFV, but they suggest that these rat sequences can raise the titer of FFV, a result analogous to their

TABLE 5. *Transmission of FFV from mass culture transformants superinfected with Mo-MuLV*

Source of Ha-MuSV nonproducer cells	FFU/ml[a]
Untransformed cells infected with Mo-MuLV	$<10^{0.3}$
Cells chronically infected with Ha-MuSV and Mo-MuLV	$10^{7.1}$
Undigested λ·Ha-MuSV (S clone)	$10^{1.3}$
*Eco*RI-digested λ·Ha-MuSV (S clone)	$10^{5.9}$
Undigested pBR322·Ha-MuSV (clone H-1)	$10^{4.7}$
*Eco*RI-digested pBR322·Ha-MuSV (clone H-1)	$10^{6.0}$
*Sal*I-digested pBR322·Ha-MuSV (clone H-1)	$10^{1.8}$
Undigested pBR322 *Pst*I fragment (clone Pst-8)	$10^{3.5}$
*Pst*I-digested pBR322 *Pst*I fragment (clone Pst-8)	$10^{4.7}$
*Sal*I-digested pBR322 *Pst*I fragment (clone Pst-8)	$10^{0.3}$

[a] Supernatant fluids were assayed for FFU and PFU after superinfection with Mo-MuLV as described in the text. All cell lines superinfected with Mo-MuLV titered at $\geq 2 \times 10^6$ PFU/ml. No FFU (<1/ml) were transmitted from transformed cells before superinfection with Mo-MuLV.

facilitative role in the DNA transfections described earlier. These variations in FFV titer were not due to an inability of the Mo-MuLV to infect the cells; the titer of Mo-MuLV was greater than 10^6 PFU/ml in all cultures.

These results obtained with the mass cultures also indicated that the form of the DNA which transformed the cells markedly affected the titer of FFV. It was also of interest to determine whether the FFV titer would be uniform or heterogeneous when transformants derived from individual foci which had been transformed by the same form of viral DNA were tested. Transformed lines derived from single-cell clones of independently induced foci (including those lines that had been analyzed above for viral RNA and p21 expression) were assayed for the efficiency with which FFV could be recovered from them after superinfection with Mo-MuLV. For this part of the study, lines transformed with undigested and *Eco*RI-digested DNA from S and M clones and with undigested clone Pst-8 and the 5'-linear clone DNA (Table 6) were used. Six days after superinfection with Mo-MuLV, FFV was recovered from all transformed cell lines, except for two derived from foci induced with the 5'-linear clone. As already suggested by the results of mass cultures, FFV was rescued from some lines with high efficiency ($\geq 10^6$ FFU/ml; "high-rescue" lines) and with low efficiency ($\leq 10^3$ FFU/ml) from others ("low-rescue" lines).

Since the Mo-MuLV-superinfected mass culture that had been transformed with the undigested S clone had a low FFV titer, it was not surprising that all 12 clonal lines transformed with undigested S and M clone DNA fell in the low-rescue category. It was very interesting to discover that although some foci transformed with *Eco*RI-digested S and M clones did possess the high-rescue phenotype seen in the superinfected mass cultures transformed with *Eco*RI-digested DNA, the majority (9 of 11 and 8 of 12 for the S and M clones, respectively) of these transformants had the low-rescue phenotype. In contrast, all clonal lines transformed with Ha-MuSV virus or with the unintegrated linear viral DNA possessed the high-rescue phenotype.

The greatly diminished efficiency (compared with virus-transformed cells) with which FFV was recovered from most lines transformed with the cloned DNA suggests that a more complex process than just pseudotyping of Ha-MuSV RNA is probably involved in this initial rescue of FFV from the low-rescue lines; once FFV had been transmitted from the low-rescue line to previously untransformed cells, the FFV was highly infectious. A second transmission to uninfected cells was found to lead to a rise in FFV titer of three to four orders of magnitude. The results from a representative low-rescue line (focus 15) and high-rescue line (focus 22) are shown in Table 7. Similar results have also been obtained with FFV rescued from cells transformed with the two subgenomic fragments (data not shown).

Structure of Ha-MuSV DNA in the transformed cells. The ability of the undigested cloned DNAs to induce foci had suggested that the viral DNA could induce foci in its cloned permuted orientation. The finding that FFV could be recovered with different levels of efficiency from superinfected transformed cell lines suggested that the structure of the viral DNA might differ in some cell lines and might be correlated with the efficiency of FFV rescue. We therefore analyzed the structure of the viral DNA in four lines transformed with the *Eco*RI-digested λ S clone (two high-rescue [foci 9 and 22] and two low-rescue [foci 14 and 15] lines) and one line (focus 28) transformed with undigested M clone DNA. Five principal theoretical arrangements of Ha-MuSV DNA might be envisioned for cells transformed by the recombinant DNAs (Fig. 6). The viral DNA might exist in the same permuted order as in the recombi-

TABLE 6. *Transmission of FFV from Ha-MuSV DNA transformants derived from individually induced foci superinfected with Mo-MuLV*

Source of Ha-MuSV NP Cells	Number of NP foci analyzed	Number of high-rescue foci (range in FFU/ml)[a]	Number of low-rescue foci (range in FFU/ml)[a]
Virus	10	10 ($10^{6.5}$ - $10^{7.3}$)	0
Unintegrated linear viral DNA	3	3 ($10^{6.6}$ - $10^{7.0}$)	0
*Eco*RI-digested λ·Ha-MuSV (S)	11	2 ($10^{6.5}$ - $10^{6.9}$)	9 ($10^{2.3}$ - $10^{2.8}$)
*Eco*RI-digested λ·Ha-MuSV (M)	12	4 ($10^{6.3}$ - $10^{6.8}$)	8 ($10^{2.3}$ - $10^{2.8}$)
Undigested λ·Ha-MuSV (S)	6	0	6 ($10^{1.0}$ - $10^{2.6}$)
Undigested λ·Ha-MuSV (M)	6	0	6 ($10^{2.3}$ - $10^{3.0}$)
Undigested clone Pst-8	4	0	4 (2×10^1 - 5×10^1)
Undigested 5'-linear clone	3	0	3[b] ($<10^{0.3}$ - 2×10^0)

[a] Conditions were as described in Table 5.

[b] FFV was recovered from only one of the three foci analyzed.

TABLE 7. *Titer of rescued FFV after first and second transmission*

Source of supernatant fluid	FFU/ml	PFU/ml
Uninfected cells	$<10^{0.3}$	$<10^{0.3}$
Mo-MuLV-infected cells	$<10^{0.3}$	$10^{6.8}$
Mo-MuLV/Ha-MuSV-infected cells	$10^{6.9}$	$10^{7.2}$
Cells transfected with *Eco*RI-digested λ·Ha-MuSV DNA:		
Focus 22 (high-rescue)		
Not superinfected	$<10^{0.3}$	$<10^{0.3}$
Superinfected with Mo-MuLV		
1st transmission	$10^{6.7}$	$10^{7.2}$
2nd transmission[a]	$10^{6.8}$	$10^{6.9}$
Focus 15 (low-rescue)		
Not superinfected	$<10^{0.3}$	$<10^{0.3}$
Superinfected with Mo-MuLV		
1st transmission	$10^{2.3}$	$10^{6.6}$
2nd transmission[a]	$10^{5.8}$	$10^{7.1}$

[a] After the first transmission of FFV to previously uninfected cells, the newly transformed cells were passaged twice, until more than 80% (estimated) of the cells were transformed. An 18-h harvest from this culture was then titered on uninfected cells for the second transmission.

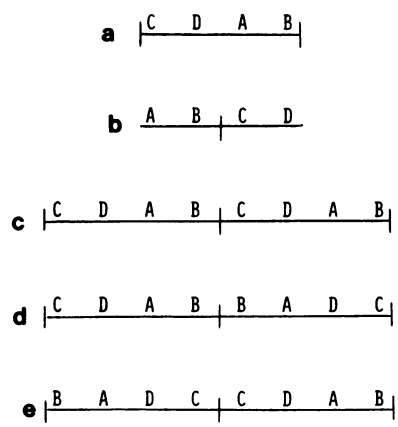

FIG. 6. *Theoretical structural organization of Ha-MuSV DNA in cells transformed by λ·Ha-MuSV DNA. The capital letters in this figure are used as in Fig. 1. The assignment of "head" and "tail" was arbitrary. (a) Single permuted molecule; (b) reoriented molecule by recircularization; (c) reoriented molecule by head-to-tail dimer; (d) head-to-head dimer; (e) tail-to-tail dimer.*

nant DNA; it might have circularized and reestablished itself in the same order as the unintegrated linear viral DNA isolated from acutely infected mouse cells; it might have formed a head-to-tail dimer of the cloned DNA—which would create one reoriented molecule—or it might have formed head-to-head or tail-to-tail dimers. Cells transformed by undigested λ·Ha-MuSV DNA would be likely to have the permuted orientation of the cloned viral DNA (since the λ DNA was still covalently linked to the Ha-MuSV DNA before transfection), whereas cells transformed by *Eco*RI-digested DNA might contain any of the above forms.

We used the Southern blotting procedure for the analysis of the structure of the viral DNA in the transformed cells. High-molecular-weight DNA was digested with three restriction enzymes: *Hin*dIII (Fig. 7A and B) and *Xba*I (Fig. 7C), which cleave the viral DNA several times, and *Bam*HI, which cleaves the viral DNA once (Fig. 7D). For the detection of viral sequences, ^{32}P-labeled Ha-MuSV DNA was synthesized in vitro by nick-translation of defined restriction endonuclease fragments from clone H-1 DNA. Two viral probes were prepared: one contained the entire Ha-MuSV DNA insert including the Mo-MuLV sequences in Ha-MuSV (the "representative" probe), and the other contained most of the rat sequences in Ha-MuSV DNA but none of the Mo-MuLV sequences (the "rat" probe). Although some Ha-MuSV sequences were not contained in the rat probe, more than 1.4 kbp on each side of the viral *Eco*RI site were present in this probe, and it is the viral sequences around the *Eco*RI site that are most critical to the analysis of the structure of the viral DNA in the transformed cells.

The high-molecular-weight DNAs in Fig. 7 are organized similarly in each panel: lane a, uninfected cells; lanes b and c, high-rescue lines; lanes d and e, low-rescue lines transformed with *Eco*RI-digested S clone DNA; lane f, Ha-MuSV virus-transformed cells; lane g, cells transformed with unintegrated linear Ha-MuSV DNA; lane h, cells transformed with undigested M clone DNA. An example of the hybridization results obtained with the representative probe is shown in Fig. 7A. In this *Hin*dIII digest of the high-molecular-weight DNAs, the uninfected cells (lane a) contained numerous bands, which suggests that the DNA from these cells already has several regions which share homology with sequences in the representative probe. Although the Ha-MuSV-transformed cells contained additional bands, the background from the endogenous cross-reacting bands and from mouse carrier DNA introduced some ambiguities in the analysis of the Ha-MuSV DNA in the transformed cells. Similar difficulties arose when the representative probe was hybridized with the high-molecular-weight DNAs digested with other enzymes (data not shown). By contrast, when the *Hin*dIII-digested DNAs were hybridized with the rat probe (Fig. 7B), the uninfected cells contained only one intense (4.3 kbp) and

one faint (1.0 kbp) band. In the Ha-MuSV-transformed cells, the new bands could be clearly separated from this limited endogenous background of cross-reacting sequences. Therefore, only the rat probe hybridization results have been shown for the other restriction enzyme digests.

Using the rat probe, *Bam*HI digestion of the DNA from cells nonproductively transformed by virus revealed a single Ha-MuSV-specific fragment (lane f); since this probe does not contain sequences to the left of the *Bam*HI site, a single band (containing the viral sequences and the right-hand virus-cell junction) implies the presence of a single copy of the viral DNA. Digestion with *Hin*dIII and with *Xba*I revealed the internal fragments of the unintegrated linear viral DNA for each enzyme (1.6 and 0.9 kbp for *Hin*dIII and 3.2 and 2.2 kbp for *Xba*I). The 3.0-kbp *Hin*dIII fragment in lane f represents the right-hand virus-cell junction fragment. These results are compatible with the conclusion that this virus-transformed cell contained a single integrated copy of Ha-MuSV DNA, which has the structure analogous to that of the unintegrated linear viral DNA, as expected, after infection with virus. Similar results were also obtained with DNA from a cell line transformed by unintegrated linear Ha-MuSV DNA (lane g). In this line, whose proviral DNA is apparently integrated at a different site, the 6.5- and 3.4-kbp bands represent the right- and left-hand virus-cell junctions, respectively.

Of the two low-rescue lines transformed by *Eco*RI-digested S clone DNA, focus 15 (lane e) probably contained two copies of viral DNA, and focus 14 (lane d) contained several copies. For focus 15, the *Hin*dIII and *Xba*I digestions indicated that the Ha-MuSV DNA was in the permuted orientation of the cloned viral DNA. In the *Hin*dIII digest, for example, an intense band comigrated with the 3.0-kbp band in the S clone (lane j); this band represents the fragment that is present in the permuted viral DNA but absent in the unintegrated linear viral DNA. Conversely, the internal 1.6-kbp *Hin*dIII fragment which is characteristic of the unintegrated linear viral DNA (and which includes the viral *Eco*RI site) was not present. The presence of two copies of viral DNA in focus 15 was inferred from the presence of four virus-specific *Bam*HI fragments, since in the permuted orientation, the rat probe should hybridize with both viral *Bam*HI fragments generated from each copy of the viral DNA. Although the low-rescue cells in lane d contained multiple copies of the viral DNA, the presence of the 3.0-kbp *Hin*dIII fragment and the absence of the 1.6-kbp *Hin*dIII fragment permitted the conclusion that at least one copy was in the permuted orientation and that no reoriented molecules were present in this line.

The two high-rescue lines transformed with *Eco*RI-digested S clone DNA contained two (focus 9, lane b) and several (focus 22, lane c) copies of viral DNA, respectively. When the focus 9 DNA was digested with *Hin*dIII, both the 3.0- and 1.6-kbp fragments were formed. This result suggested that both a reoriented molecule and a permuted molecule were present in this line, either by recircularization of a molecule or by head-to-tail dimer formation. If the reoriented molecule were the result of a head-to-tail dimer of the permuted DNA, digestion with *Bam*HI (which cleaves the viral DNA once) should yield a 5.4-kbp fragment, as was observed (arrow, Fig. 7D, lane b). In data not shown, *Pvu*I (a second enzyme that cleaves viral DNA at a single site [R. Ellis, unpublished data]) digestion also gave a 5.4-kbp fragment; digestion with *Hpa*I (which does not cleave Ha-MuSV) yielded a single 20-kbp fragment. These results therefore strongly suggested that the viral DNA is present as a head-to-tail dimer in this high-rescue cell line.

Although the other high-rescue cell line analyzed (lane c) contained several copies of the viral DNA, this DNA was interesting because in the *Hin*dIII digest it contained, in addition to the 3.0-kbp band, an intense 1.4-kbp band (rather than the expected 1.6-kbp band). This band probably represents a deleted form of the sequences in the 1.6-kbp fragment; after rescue of Ha-MuSV from this line, the unintegrated linear viral DNA is 0.2 kbp shorter than wild-type Ha-MuSV DNA, it lacks the *Eco*RI site, and it contains a 1.4-kbp *Hin*dIII fragment rather than the 1.6-kbp fragment (unpublished data). If this cell line were to contain a head-to-tail dimer, digestion with an enzyme which cleaved the viral DNA once should yield a 5.2-kbp band (as a result of the 0.2-kbp deletion around the *Eco*RI site). Such a band was found after *Bam*HI digestion (Fig. 7D, lane c). The results indicate that at least one copy of the viral DNA in these high-rescue cells was in the same orientation as the DNA in virus-transformed nonproducer cells. They further suggest that this reorientation of the cloned DNA arose through the formation of a head-to-tail dimer, which in this instance deleted 0.2 kbp surrounding the *Eco*RI site.

The cells transformed with undigested M clone DNA (lane h) contained two viral DNA molecules. Because of the orientation of this Ha-MuSV insert with the λ DNA and the known locations of the *Bam*HI sites in the λ DNA, *Bam*HI digestion should yield 6.6- and 18.2-kbp Ha-MuSV fragments, if the λ·Ha-MuSV DNA

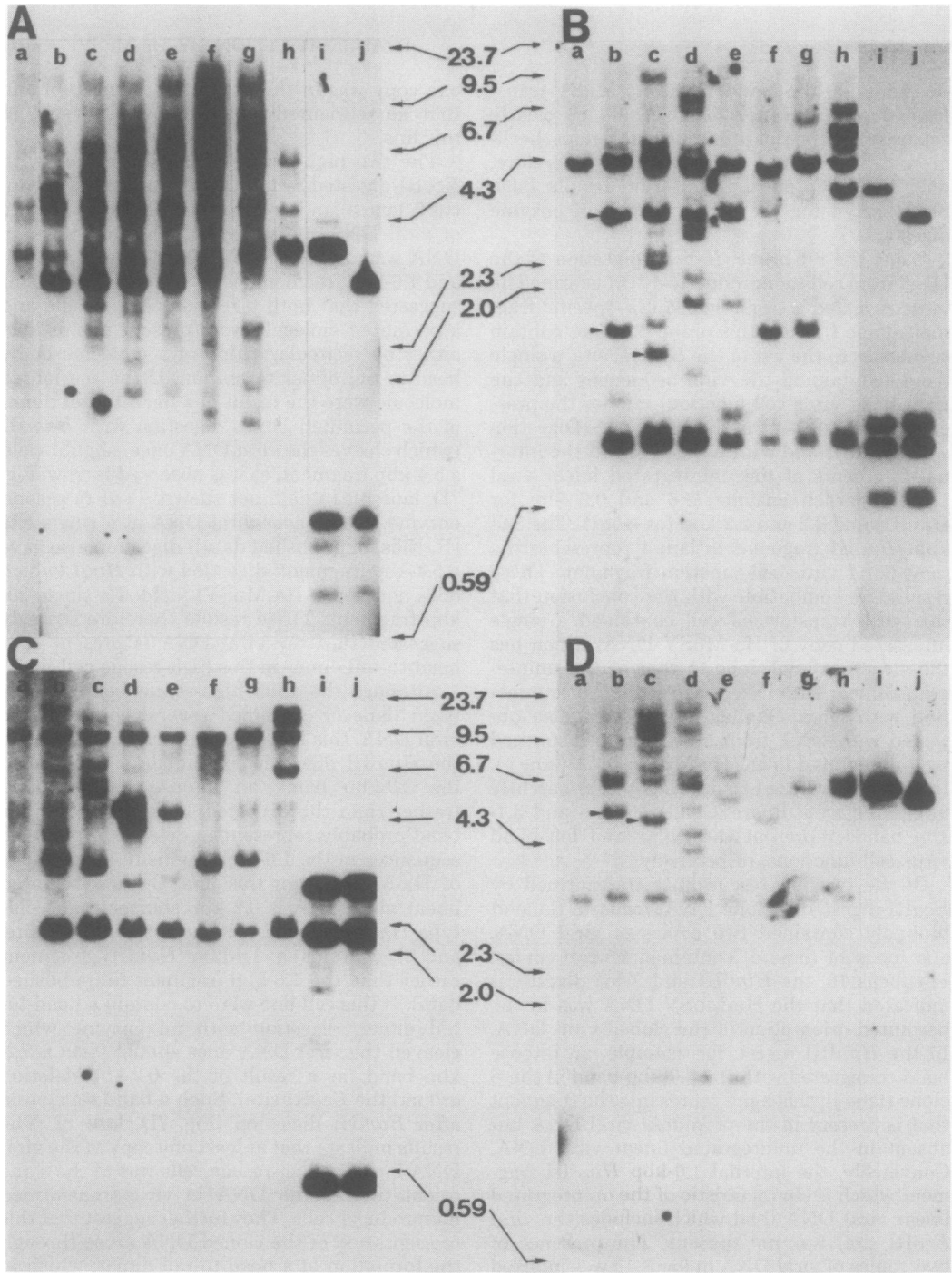

FIG. 7. *Agarose gel electrophoresis of restriction endonuclease-digested high-molecular-weight DNA from Ha-MuSV-transformed cells. A 15-μg sample of digested DNA was subjected to electrophoresis in 1% agarose, blotted onto nitrocellulose filters, and hybridized to Ha-MuSV [^{32}P]DNA. (A) HindIII-digested DNAs hybridized to the representative Ha-MuSV DNA probe; (B) HindIII-digested DNAs hybridized to the rat probe; (C) XbaI-digested DNAs hybridized to the rat probe; (D) BamHI-digested DNAs hybridized to the rat probe. Lanes: (a) NIH 3T3 uninfected cells; (b and c) focus 9 and focus 22, high-rescue lines; (d and e) focus 14 and focus 15, low-rescue lines; (f) focus 13, Ha-MuSV-transformed nonproducer; (g) focus 7, Ha-MuSV unintegrated linear DNA-transformed nonproducer; (h) focus 19, vector-Ha-MuSV-transformed undigested nonproducer; (i) EcoRI-digested λ·Ha-MuSV DNA (3 ng of the M clone); (j) EcoRI-digested λ·Ha-MuSV DNA (3 ng of the S clone). The arrows next to the panels refer to the location of ^{32}P-labeled HindIII marker wild-type λ DNA (length given in kilobase pairs) electrophoresed with each gel. The upper part of the*

were intact between the λ *Bam*HI sites. Both of these bands as well as a 6.0-kbp band were visualized. As expected for Ha-MuSV DNA covalently linked to λ DNA when the *Bam*HI-digested DNA was hybridized with a λ [^{32}P]-DNA probe a λ-specific band comigrated with each Ha-MuSV-specific band (data not shown). When the DNA from this cell line was digested with *Hin*dIII, a 3.6-kbp Ha-MuSV-specific fragment, which comigrated with the large *Hin*dIII fragment of the M clone (Fig. 7B, lane i), was present, and the 1.6-kbp *Hin*dIII fragment was absent. These results indicated that this cell contained Ha-MuSV DNA in the permuted order of the cloned Ha-MuSV DNA which was covalently linked to the λ DNA.

DISCUSSION

As noted in the Introduction, Ha-MuSV is a recombinant between Mo-MuLV and endogenous rat genetic sequences. The 4.5-kbp rat insert falls into two categories: the 3′ half contains extensive homology with the endogenous rat 30S sequences (6, 45), which are nontransforming type C virus-related sequences expressed in a variety of rat cells (40, 49), and the 5′ half shares little homology with these sequences (R. W. Ellis et al., submitted for publication). The current studies utilizing cloned Ha-MuSV DNA have begun to assign specific functions to different parts of the viral genome.

The ability of DNA from the 5′-linear clone and from clone Pst-8 to induce transformation of NIH 3T3 cells indicated that the transforming function of the virus must be located within the 2.3 kbp closest to the 5′ end of the unintegrated linear viral DNA, since this was the region of overlap between the two clones (see Fig. 2). This region includes the 0.5 kbp of the ETR derived from the 3′ end of the viral RNA and 1.8 kbp derived from the 5′ end, but we do not believe that the ETR is absolutely required for transformation; subgenomic fragments of Mo-MuSV DNA which lack ETR have already been shown to induce transformation (1, 32). The liquid hybridizations with the transformed lines eliminated the unlikely theoretical possibility that expression of the 3′ sequences in the ETR was required for maintenance of the transformed phenotype, since RNA levels from the 3′ end of the viral RNA in some transformants were no higher than the levels in uninfected cells. By contrast, all the transformants contained high levels of RNA derived from the 5′ region of the viral genome. At saturation, RNA from a Pst-8-induced transformant hybridized fewer counts than did the other transformants, since the insert in clone Pst-8 lacked 40% of the sequences contained in the 5′ probe. These results suggested that transformation by Ha-MuSV was encoded by sequences contained within the 1.8 kbp closest to the 5′ end of the viral RNA. The

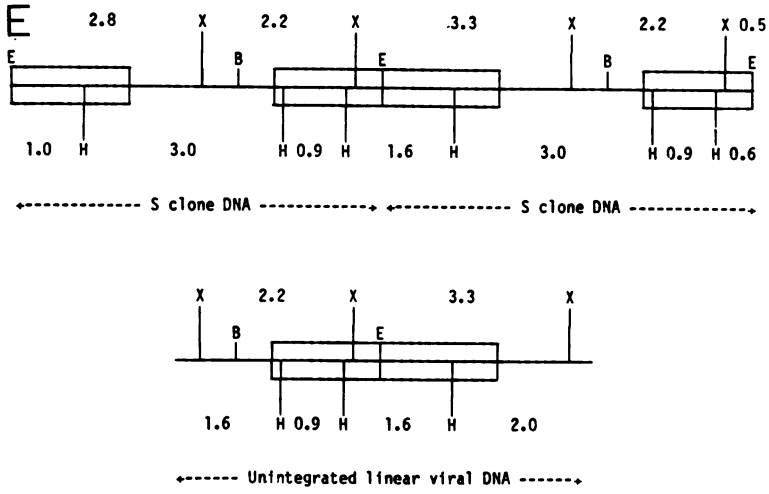

schematic diagram represents the structure of a head-to-tail dimer of the S clone DNA joined at the EcoRI site. The lower part of the diagram represents the structure of unintegrated linear viral DNA. The letters refer to the restriction enzyme sites in these DNAs: B, BamHI; E, EcoRI; H, HindIII; X, XbaI. The numbers represent the distances (in kilobase pairs) between the enzyme sites. The rectangles represent the sequences contained in the rat probe.

data are also compatible with the hypothesis that the ETR may be a strong promoter for viral RNA transcription.

The sequences that encode the viral p21 have also been localized to the transforming region of the viral genome, since all the transformants (including those induced with DNA from clone Pst-8) contained p21 which was qualitatively and functionally (as measured by the GDP-binding assay) indistinguishable from the authentic viral p21. Except for 50 to 100 nucleotides at the 5′ end of the viral RNA, this region is composed entirely of rat sequences. Therefore, p21 (a minimum of about 600 nucleotides) is most likely encoded by the rat sequences. The location of the p21 coding sequences near the 5′ end of the viral RNA is consistent with previous translation studies, which showed that p21 was synthesized in highest amounts from full-length Ha-MuSV RNA (43). Since this region of Ha-MuSV apparently shares little homology with the rat 30S sequences, it is probable that most of the p21 coding sequences are not derived from the 30S sequences. It has recently been determined that the p21 was required for maintenance of transformation, since the protein was thermolabile in a Ki-MuSV mutant which was temperature sensitive for the maintenance of transformation (44). This biological activity of p21 and the localization of its coding sequences to the transforming region of the viral genome have led us to conclude that the p21 represents the *src* gene product of Ha-MuSV and Ki-MuSV.

The 5′ location of the p21 contrasts with the 3′ location of the transforming regions of Mo-MuSV (1) and of Rous sarcoma virus (51) and its *src* gene product (p60) (4, 11). These results suggest that the location of transforming regions of retroviruses may be heterogeneous. On the other hand, the localization of the *src* region in Ha-MuSV to the rat insert is similar to the *src* regions of Rous sarcoma virus and Mo-MuSV, which also represent cell sequence inserts in helper-independent viral genomes (12, 36, 47).

The rat sequences on the 3′ side of the *src* region, the area that shares considerable homology with the endogenous 30S sequences, are clearly not absolutely required either for the induction of transformation by Ha-MuSV or its rescue from superinfected cells. M. P. Goldfarb and R. A. Weinberg (personal communications) have independently made the same observation. There are, however, some data which suggest that this region facilitates the transforming activity of transfected viral DNA and raises the titer of virus rescued from cells transformed with the cloned DNA. The transforming efficiency of clone Pst-8, which was missing 1.5 kbp from this region of the genome, was one order of magnitude less than the transforming efficiency of the complete permuted genome (clone H-1). Whether this facilitation is only due to size differences or is related to specific rat sequences remains to be determined. The observation that transforming efficiency of clone Pst-8 was not affected by digestion with *PstI* suggests that the pBR322 sequences cannot substitute for the rat sequences. These rat sequences also affected the recovery of virus from superinfected transformed cells. The 6-day titer of virus recovered from mass cultures transformed with clone Pst-8 as the undigested circular DNA, after linearization of the DNA by cleavage at the pBR322 *SalI* site, or after separation of the viral DNA from the vector, was lower than that recovered from cells transformed with the analogous forms of clone H-1. These results suggest that although the sequences near the middle of the viral genome are not absolutely required for rescue of virus, they facilitate this biological property of the virus.

Another indication of the enhancing function of the nontransforming regions is seen in earlier transfection studies of Ha-MuSV DNA. It has been noted previously that *Eco*RI digestion of the unintegrated linear viral DNA markedly decreased its infectivity (14, 27). This decrease in infectivity had initially suggested to us that the viral *Eco*RI site might represent part of the transforming region, but that is clearly not the case. It now seems more likely that this decreased infectivity is due principally to separation of the *src* coding sequences of Ha-MuSV from the ETR at the 3′ end of the unintegrated linear viral DNA, since it is probable that the integrity of the terminal sequences at both ends of the viral genome accounts in large part for the high infectivity of this molecular species.

The virus rescue studies demonstrated that efficient transmission of FFV to uninfected cells occurred only when the viral genome was oriented as in the form of the viral genome in virus-transformed nonproducer cells. Ha-MuSV was rescued with high efficiency from clonal lines transformed with either Ha-MuSV virus or the unintegrated linear viral DNA; these transformants contained integrated viral DNA which had the form of the unintegrated linear viral DNA. Although Ha-MuSV was rescued with high efficiency from mass cultures transformed by *Eco*RI-digested Ha-MuSV DNA cloned in λ or in pBR322, analysis of cloned lines derived from individual foci which had been transformed with the S and M clones indicated that Ha-MuSV was rescued with high efficiency from only a minority of the cell lines. Virus was rescued with much lower efficiency from the other cell lines transformed by *Eco*RI-digested S and M clone

DNA and from each of the lines transformed with undigested S and M clone DNA.

Biochemical analysis of five lines transformed with λ·Ha-MuSV DNA indicated that Ha-MuSV DNA was oriented as in virus-transformed cells in both lines from which Ha-MuSV was rescued with high efficiency, whereas it was in the permuted orientation in the three cell lines from which virus was rescued with low efficiency. Although it is probable that reorientation of the viral DNA can occur either by recircularization of the permuted *Eco*RI Ha-MuSV insert or by the formation of a head-to-tail dimer of the insert, the two clones that have been analyzed appear to contain head-to-tail dimers. Since viral DNA in cells transformed with the undigested DNA was covalently linked to λ DNA, it was in the permuted form.

Our results suggest that efficient transmission of FFV requires the nonpermuted orientation present in cells transformed by virus, probably because the ETR is then at each end of the viral DNA, thus permitting transcription of an intact RNA molecule. Cells that contain the viral DNA in its permuted form are apparently as transformed as those with the nonpermuted orientation. However, the ability to transmit from them is markedly impaired even when the Ha-MuSV is not covalently linked to λ DNA or when sequences from the 3′ end of the molecule are being expressed as RNA, as was found in two low-rescue lines transformed with undigested recombinant DNA. No obvious correlation has been noted between the number of copies of Ha-MuSV DNA and either the degree to which the cells have been transformed or the efficiency with which virus was rescued. The permuted orientation of the viral DNA in the low-rescue clones, combined with the lack of detectable RNA expression from the 3′ end in some of them, suggests that the recovery of FFV from these cells by Mo-MuLV is probably a more complex process than simple pseudotyping of viral RNA. The relatively high infectivity of second-passage FFV suggests that the low efficiency step lies in the initial transmission of the FFV. One possibility is that the transforming sequences may recombine with the superinfecting Mo-MuLV to regenerate a Mo-MuLV 3′ end. This and other hypotheses are currently being evaluated.

ACKNOWLEDGMENTS

We thank W. L. McClements for helpful discussion and L. Shaughnessy for typing the manuscript.

This work was supported in part by a contract from the National Cancer Institute to Meloy Laboratories, Springfield, Va.

LITERATURE CITED

1. **Andersson, P., M. P. Goldfarb, and R. E. Weinberg.** 1979. A defined subgenomic fragment of in vitro synthesized Moloney sarcoma virus DNA can induce cell transformation upon transfection. Cell **16**:63–75.
2. **Bishop, J. M.** 1978. Retroviruses. Annu. Rev. Biochem. **47**:35–88.
3. **Bolivar, F., R. L. Rodriguez, P. J. Greene, M. C. Betlach, H. L. Heyneker, and H. W. Boyer.** 1977. Construction and characterization of new cloning vehicles. II. A multipurpose cloning system. Gene **2**:95–113.
4. **Brugge, J. S., and R. L. Erikson.** 1977. Identification of a transformation-specific antigen induced by an avain sarcoma virus. Nature (London) **269**:346–348.
5. **Chan, H. W., C. F. Garon, E. H. Chang, D. R. Lowy, G. L. Hager, E. M. Scolnick, R. Repaske, and M. A. Martin.** 1980. Molecular cloning of the Harvey sarcoma virus circular DNA intermediates. II. Further structural analyses. J. Virol. **33**:845–855.
6. **Chien, Y. H., M. Lai, T. Y. Shih, I. M. Verma, E. M. Scolnick, P. Roy-Burman, and N. Davidson.** 1979. Heteroduplex analysis of the sequence relationships between the genomes of Kirsten and Harvey sarcoma viruses, their respective parental murine leukemia viruses, and the rat endogenous 30S RNA. J. Virol. **31**: 752–760.
7. **Coffin, J. M., T. C. Hageman, A. M. Maxam, and W. A. Haseltine.** 1978. Structure of the genome of Moloney murine leukemia virus: a terminally redundant sequence. Cell **13**:761–774.
8. **Cohen, S. N., A. C. Y. Chang, and L. Hsu.** 1972. Nonchromosomal antibiotic resistance in bacteria: general transformation of *Escherichia coli* by R-factor DNA. Proc. Natl. Acad. Sci. U.S.A. **69**:2110–2114.
9. **Colman, A., M. J. Byers, S. B. Primrose, and A. Lyons.** 1978. Rapid purification of plasmid DNAs by hydroxyapatite chromatography. Eur. J. Biochem. **91**: 303–310.
10. **Department of Health, Education and Welfare, National Institutes of Health.** 1979. Recombinant DNA research, part II. Fed. Regist. **44**:21730–21736.
11. **Erikson, E., M. S. Collett, and R. L. Erikson.** 1978. In vitro synthesis of a functional avain sarcoma virus transforming gene product. Nature (London) **274**:919–921.
12. **Frankel, A. E., R. L. Neubauer, and P. J. Fischinger.** 1976. Fractionation of nucleotide transcripts from Moloney sarcoma virus and isolation of sarcoma virus-specific complementary DNA. J. Virol. **18**:481–490.
13. **Gilboa, E., S. Goff, A. Shields, F. Yoshimura, S. Mitra, and D. Baltimore.** 1979. In vitro synthesis of a 9 kbp terminally redundant DNA carrying the infectivity of Moloney murine leukemia virus. Cell **16**:863–874.
14. **Goldfarb, M. F., and R. A. Weinberg.** 1979. Physical map of the biologiacally active Harvey sarcoma virus unintegrated linear DNA. J. Virol. **32**:30–39.
15. **Graham, F. L., and A. J. van der Eb.** 1973. Transformation of rat cells by DNA of human adenovirus 5. Virology **52**:456–461.
16. **Gross-Bellard, M., P. Oudet, and P. Chambon.** 1973. Isolation of high-molecular-weight DNA from mammalian cells. Eur. J. Biochem. **36**:32–38.
17. **Grunstein, M., and D. S. Hogness.** 1975. Colony hybridization: a method for the isolation of cloned DNAs that contain a specific gene. Proc. Natl. Acad. Sci. U.S.A. **72**:3961–3965.
18. **Hager, G. L., E. H. Chang, H. W. Chan, C. F. Garon, M. A. Israel, M. A. Martin, E. M. Scolnick, and D. R. Lowy.** 1979. Molecular cloning of the Harvey sarcoma virus closed circular DNA intermediates: initial structural and biological characterization. J. Virol. **31**: 795–809.
19. **Hanafusa, H.** 1977. Cell transformation by RNA tumor viruses. Compr. Virol. **10**:401–483.
20. **Harvey, J. J.** 1964. An unidentified virus which causes the rapid production of tumors in mice. Nature (Lon-

don) 204:1104–1105.
21. **Hirt, B.** 1967. Selective extraction of polyoma DNA from infected mouse cell cultures. J. Mol. Biol. **26**:365–369.
22. **Hsu, T. W., J. L. Sabran, G. E. Mark, R. V. Guntaka, and J. M. Taylor.** 1978. Analysis of unintegrated avian RNA tumor virus double-stranded DNA intermediates. J. Virol. **28**:810–818.
23. **Hughes, S. H., P. R. Shank, D. H. Spector, H. J. Kung, J. M. Bishop, H. E. Varmus, P. K. Vogt, and M. L. Breitman.** 1978. Proviruses of avian sarcoma virus are terminally redundant, coextensive with unintegrated linear DNA and integrated at many sites. Cell **15**:1397–1410.
24. **Kirsten, W. H., and L. A. Mayer.** 1967. Morphologic responses to a murine erythroblastosis virus. J. Natl. Cancer Inst. **39**:311–319.
25. **Jainchill, J. F., S. A. Aaronson, and G. J. Todaro.** 1969. Murine sarcoma and leukemia viruses: assay using clonal lines of contact-inhibited mouse cells. J. Virol. **4**: 549–553.
26. **Leder, P., D. Tiemeier, and L. Enquist.** 1977. EK2 derivatives of bacteriophage lambda useful in the cloning of DNA from higher organism: the λgtWES system. Science **196**:175–177.
27. **Lowy, D. R., E. Rands, and E. M. Scolnick.** 1978. Helper-independent transformation by unintegrated Harvey sarcoma virus DNA. J. Virol. **26**:291–298.
28. **Lowy, D. R., and E. M. Scolnick.** 1978. Glucocorticoids induce focus formation and increase sarcoma viral expression in a mink cell line that contains a murine sarcoma viral genome. J. Virol. **25**: 157–163.
29. **Maisel, J., E. M. Scolnick, and P. Duesberg.** 1975. Base sequence differences between the RNA components of Harvey sarcoma virus. J. Virol. **16**:749–753.
30. **Maniatis, T., A. Jeffrey, and D. G. Kleid.** 1975. Nucleotide sequence of the rightward operator of phage λ. Proc. Natl. Acad. Sci. U.S.A. **72**:1184–1188.
31. **McDonell, M. W., M. N. Simon, and F. W. Studier.** 1977. Analysis of restriction fragments of T_7 DNA and determination of molecular weights by electrophoresis in neutral and alkaline gels. J. Mol. Biol. **110**:119–146.
32. **Oskarsson, M., W. L. McClements, D. L. Blair, G. F. Vande Woude, and J. V. Maizel.** 1980. Properties of a normal mouse cell DNA sequence (*sarc*) homologous to the *src* sequence of Moloney sarcoma virus. Science **207**:1222–1224.
33. **Pearson, R. L., J. F. Weiss, and A. D. Kelmers.** 1971. Improved separation of transfer RNAs on polychlorotrifluoroethylene-supported reversed-phase chromatography columns. Biochim. Biophys. Acta **228**:770–774.
34. **Rowe, W. P., W. E. Pugh, and J. W. Hartley.** 1970. Plaque assay techniques for murine leukemia viruses. Virology **42**:1136–1139.
35. **Sabran, J. L., T. W. Hsu, C. Yeater, A. Kaji, W. S. Mason, and J. M. Taylor.** 1979. Analysis of integrated avain RNA tumor virus DNA in transformed chicken, duck, and quail fibroblasts. J. Virol. **29**:170–178.
36. **Scolnick, E. M., R. S. Howk, A. Anisowizc, P. T. Peebles, C. D. Sherr, and W. P. Parks.** 1975. Separation of sarcoma virus-specific and leukemia virus-specific genetic sequences of Moloney sarcoma virus. Proc. Natl. Acad. Sci. U.S.A. **72**:4650–4654.
37. **Scolnick, E. M., A. G. Papageorge, and T. Y. Shih.** 1979. Guanine nucleotide-binding activity as an assay for src protein of rat-derived murine sarcoma viruses. Proc. Natl. Acad. Sci. U.S.A. **76**:5355–5359.
38. **Scolnick, E. M., and W. P. Parks.** 1974. Harvey sarcoma virus: a second murine type-C sarcoma virus with rat genetic information. J. Virol. **13**:1211–1219.
39. **Scolnick, E. M., E. Rands, D. Williams, and W. P. Parks.** 1973. Studies on the nucleic acid sequences of Kirsten sarcoma virus: a model for the formation of a mammalian RNA-containing sarcoma virus. J. Virol. **12**:458–463.
40. **Scolnick, E. M., W. C. Vass, R. S. Howk, and P. H. Duesberg.** 1979. Defective retrovirus-like 30S RNA species of rat and mouse cells are infectious if packaged by type C helper virus. J. Virol. **29**:964–972.
41. **Shank, P. R., S. H. Hughes, H.-J. Kung. J. E. Majors, W. Quintrell, R. V. Guntaka, J. M. Bishop, and H. E. Varmus.** 1978. Mapping unintegrated avain sarcoma virus DNA: termini of linear DNA bear 300 nucleotides present once or twice in two species of circular DNA. Cell **15**:1383–1395.
42. **Sharp, P. A., B. Sugden, and J. Sambrook.** 1973. Detection of two restriction endonuclease activities in Haemophilus parainfluenzae using analytical agarose ethidium bromide electrophoresis. Biochemistry **12**: 3055–3063.
43. **Shih, T. Y., M. O. Weeks, H. A. Young, and E. M. Scolnick,** 1979. Identification of a sarcoma virus coded phosphoprotein in nonproducer cells transformed by Kirsten or Harvey murine sarcoma virus. Virology **96**: 64–79.
44. **Shih, T. Y., M. O. Weeks, H. A. Young, and E. M. Scolnick.** 1979. P21 of Kirsten murine sarcoma virus is thermolabile in a viral mutant temperature sensitive for the maintenance of transformation. J. Virol. **31**:546–556.
45. **Shih, T. Y., D. R. Williams, M. O. Weeks, J. M. Maryak, W. C. Vass, and E. M. Scolnick.** 1978. Comparison of the genomic organization of Kirsten and Harvey sarcoma viruses. J. Virol. **27**:45–55.
46. **Southern, E. M.** 1975. Detection of specific sequences among DNA fragments separated by gel electrophoresis. J. Mol. Biol. **38**:503–517.
47. **Stehelin, D., R. V. Guntaka, H. E. Varmus, and J. M. Bishop.** 1976. Purification of DNA complementary to nucleotide sequences required for neoplastic transformation of fibroblasts by avain sarcoma viruses. J. Mol. Biol. **101**:349–365.
48. **Svoboda, J., P. P. Chyle, D. Simkovic, and I. Hilgert.** 1963. Demonstration of the absence of infectious Rous virus in rat tumor XC whose structuraly intact cells produce Rous sarcoma when transferred to chicks. Folia Biol. **9**:77–81.
49. **Tsuchida, N., R. Gilden, and M. Hatanaka.** 1974. Sarcoma virus-related RNA sequence in normal rat cells. Proc. Natl. Acad. Sci. U.S.A. **71**:4503–4507.
50. **Vogt, P. K.** 1977. Genetics of RNA tumor viruses. Compr. Virol. **9**:341–455.
51. **Wang, L.-H., P. Duesberg, K. Beemon, and P. K. Vogt.** 1975. Mapping RNase T_1-resistant oligonucleotides of avain tumor virus RNAs: sarcoma-specific oligonucleotides are near the poly(A) end and oligonucleotides common to sarcoma and transformation-defective viruses are at the poly(A) end. J. Virol. **16**: 1051–1070.
52. **Yoshimura, F. K., and R. A. Weinberg.** 1979. Restriction endonuclease cleavage of linear and closed circular murine leukemia viral DNAs: discovery of a smaller circular form. Cell **16**:323–332.